Advances in Nanoparticles, 2015, 4, 37-44
Published Online May 2015 in SciRes. http://www.scirp.org/journal/anp
http://dx.doi.org/10.4236/anp.2015.42005

Effect of Sintering Temperature on $Co_{0.5}Zn_{0.5}Fe_2O_4$ Nano-Particles Evolution and Particle Size Distribution

Abubakar Yakubu[1], Zulkifly Abbas[1], Mansor Hashim[2], Ahmad Fahad[3]

[1]Department of Physics, Faculty of Science, Universiti Putra Malaysia, Selangor, Malaysia
[2]Institute of Advance Technology and Material Science (ITMA), Universiti Putra Malaysia, Selangor, Malaysia
[3]Institute of Mathematical Research (INSPEM), Universiti Putra Malaysia, Selangor, Malaysia
Email: abulect73@yahoo.com

Received 25 August 2014; accepted 4 May 2015; published 8 May 2015

Abstract

This study involves an investigation to ascertain the effect of sintering temperature on the particle size distribution of $Co_{0.5}Zn_{0.5}Fe_2O_4$ nano-particle. The effect of the sintering temperature towards diffusion of CoO and ZnO into the tetrahedral and octahedral sites was also reported. In this study, CoO, ZnO and Fe_2O_3 powders were mechanically alloyed to synthesize fine powders of $Co_{0.5}Zn_{0.5}Fe_2O_4$ nano-particles. The synthesized powder was then sintered at various temperatures which were employed to study the effect of sintering temperature on the materials. Further analysis was done using XRD to investigate the phases of the powder and the crystallite size using Scherrer equation, SEM and EDX for the morphology and elemental composition of samples. The XRD spectra indicated that Both ZnO and CoO powder reacted well during sintering, however, ZnO was first to diffuse into its crystallographic sites before CoO. While the particle size distribution increases as the sintering temperature increases. Amongst other findings, it was confirmed that sintering temperature affects the particle size distribution of samples and samples begin to agglomerate at temperature above 700˚C.

Keywords

Sintering, Temperature, Mechanical Alloy, Agglomerate, Nanoparticles

1. Introduction

The useful properties of soft ferrites in low and high-frequency equipment and their roles in microwave devices,

How to cite this paper: Yakubu, A., Abbas, Z., Hashim, M. and Fahad, A. (2015) Effect of Sintering Temperature on $Co_{0.5}Zn_{0.5}Fe_2O_4$ Nano-Particles Evolution and Particle Size Distribution. *Advances in Nanoparticles*, **4**, 37-44.
http://dx.doi.org/10.4236/anp.2015.42005

power transformers, rod antennas, read/write heads for high speed digital tapes have attracted much interest for researchers [1]. Soft ferrites are divided into two major categories; the manganese-zinc (MnZn) ferrite and the nickel-zinc (NiZn) ferrite. However, in the recent, CoZn ferrite has blossom in researches involving high frequency devices. Soft ferrites can be used in the areas of low and high frequency devices, microwave devices, power transformers, read/write heads, antennas for communication and for interference suppression and absorption. The advantages of using soft ferrites are listed as follows:

Small eddy current loss at high frequency, chemical stability, high resistivity, low dielectric losses and high permeability, wide range of operating frequencies, low cost, light weight, large material selection, high Curie temperature.

The electromagnetic properties of ferrites materials are highly dependent on a number of factors. These factors include preparation techniques, temperature, and purity of materials used in sample preparation. In a number of researches under taken, polycrystalline sample $BiFeO_3$ synthesized at low temperature showed that the crystallite size increases and strain in the crystallite decreases with increasing sintering temperature thereby decreasing the lattice parameter [2].

Polycrystalline $NiFe_2O_4$ was prepared by solid state reaction from nano size powder of NiO and Fe_2O_3 which were synthesized by wet chemical method [3]. This method produced an inverse spinel single phase which was confirmed by the X-ray diffraction patterns. SEM micrographs of the prepared samples showed that the grain size increases with increasing sintering temperature.

In [4], they prepared nano zinc niobate powder using high energy ball milling; the powders produced were further sintered at different temperatures. Samples prepared at temperatures ranges of 975˚C to 1100˚C, exhibited a single columbite phase with a relative densities range of 87% to 99%.

Ferrites are manufactured by processing a composition of iron oxide mixed with other major constituents such as oxides or carbonates of either manganese and zinc, nickel and zinc, cobalt and zinc. The basic process is common to most ceramic process technologies and can be divided into four major functions: powder synthesis, pelletization, sintering and finishing [5] [6]. This study intends to explore the impact of the sintering temperature on the microstructure of the Co-Zn ferrite since the electromagnetic properties are very sensitive to their micro-structure.

Among the current methods for synthesis of cobalt-zinc ferrite, the mechanical alloy technique stands as a good candidate for large scale production nano ferrites. The mechanical alloy method is quite easy, fast, and inexpensive, and above all friendly to the environment.

In this study, CoO + ZnO + Fe_2O_3 were mixed together and milled for 12 hours using high energy milling machine before they are sintered for 10 hours with different sintering temperature. The sintered samples are then used to study the changes on its structural properties.

2. Method

$Co_{0.5}Zn_{0.5}Fe_2O_4$ was prepared by mechanical alloying technique using the normal combination of iron oxide and other major constituents (Co-Zn). Materials used for the production of nano ferrite in this study are Fe_2O_3 (Alfa Aesar) (99.95%), CoO (Alfa Aesar) (99.99%) and ZnO (Alfa Aesar) (99.99%). High energy milling was carried out in a SPEX 8000D shaker for 12 hours. The ball to powder mass ratio used was 10:1. The milled powder was then prepared into rectangular pellets of 3 mm, 5 mm and 7 mm thick, which was further used for dielectric characterization not mentioned in this paper. The powder and pellets were then sintered at temperatures of 500˚C, 700˚C, 900˚C and 1100˚C for 10 hours each respectively.

X-ray diffraction (Phillips Expert MPD System) coupled with graphite monochromator, operating at 40 kV and 30 mA using CuKα radiation (λ = 0.1542 nm) at a scan rate of 0.332 θ/sec was used to analyse all samples used in this study. The different samples sintered at different temperatures were analysed with Scanning Electron Microscope (SEM), Transmission electron microscope (TEM), and Energy Dispersive X ray (EDX).

3. Results and Discussion

X-ray patterns of the synthesized samples of $Co_{0.5}Zn_{0.5}Fe_2O_4$ as burnt powders and sintered at different temperatures are shown in **Figure 1**. Observation on the XRD result for sintered sample at 500˚C showed that Co-Zn ferrite existed as a major phase and ZnO as a minor phase. Analysis shows that the zinc ions do not react in the formation of the ferrite. No additional phase was detected as the sintering temperature begins to increase

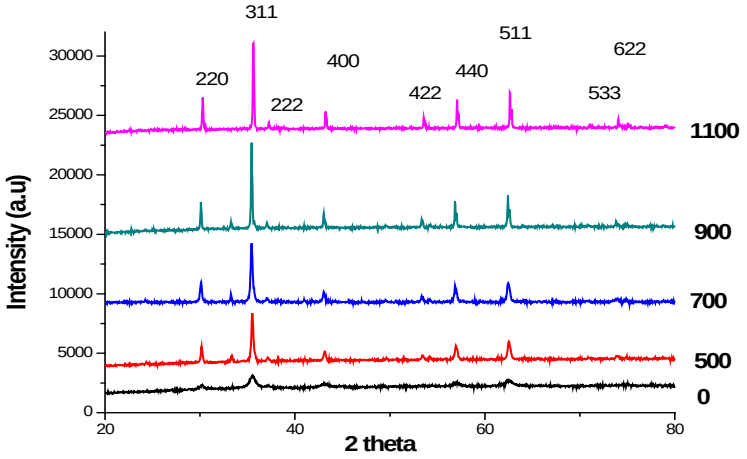

Figure 1. XRD spectra of Co-Zn-ferrites powder prepared by mechanical alloying at different sintering temperatures.

and single phase spinel structure resulted as a result of the sintering [7]. Observations on the XRD pattern for the 900˚C and 1100˚C showed strains (**Figure 1**) which might be attributed to remnant stress through chemical reaction process [8] [9]. The small crystallite sizes of samples are evident from the broad peaks patterns as shown in **Figure 1** [10].

The interpretation of the XRD spectra for all sintering temperatures was achieved using the data base of the Joint Committee on Powder Diffraction Standards [11]. Scherer equation was employed in the calculation of the crystallite size of powders under study shown in Equation (1) [12].

$$D = \frac{k\lambda}{\beta\cos\theta} \tag{1}$$

where D is the crystallite size, k is shape factor, λ is X-ray wavelength, β is full-wave half maximum in radians.

Analysis showed that the average grain size increased with increasing sintering temperature. In [13], they stated that Zn promotes sintering and hence increases the grain size as the temperature increases.

As expected, between the temperature ranges of 700˚C to 1100˚C complete phase of $Co_{0.5}Zn_{0.5}Fe_2O_4$ begins to emanate with increasing peaks as the sintering temperature increases. Careful observation on **Figure 1**, showed that at 1100˚C, some strange peaks begin to appear. These new peaks at the (533) and (622) might be attributed to transition from the single spinel phase to the magnetisation phase and the loss of Zn^{2+} at higher sintering temperature. Zn^{2+} loss due to high temperature will result in stoichiometry imbalance which causes the Fe^{3+} ions to be converted to Fe^{2+} ions which in turn will lead to electrical charge balance of material composition [14].

Increasing sintering temperature influences the increase in lattice parameter of samples which in turn causes the diffusion of zinc ions in to the tetrahedral sites of the samples. This assertion is supported by research undertaken by [15].

As the sintering temperature increases for the milled powder, the intensity of all the samples also increases as evident in **Table 1**. Table is the summary the intensity as sintering temperature increases.

The lattice constant is calculated from the combination of the Bragg's equation and d-spacing expression for cubic system (Equation (2)) [12].

$$\frac{4\sin^2\theta}{\lambda^2} = \frac{h^2+k^2+l^2}{x^2} \tag{2}$$

where x is the lattice constant, and h, k, l are the peak numbers, λ is X ray wave number.

The lattice constants was calculated using Equation (2). The magnitudes of lattice parameter for the different sintering temperatures were obtained as 8.389 Å, 8.405 Å, 8.386 Å, 8.403 Å, and 8.361 Å for the 0˚C, 500˚C, 700˚C, 900˚C, and 1100˚C temperatures respectively. The irregular behaviour of the lattice parameter might be due to the initial change in evolution in grain growth and crystallization [16] [17]. The diffusion of zinc ions into the tetrahedral sites are the main causes of the change in lattice parameter of samples, due to sintering.

The X ray density (D_x) of samples were calculated using the given equation in (3), [12]

$$D_x = \frac{8 \times M}{N \times a^3} \text{g} \cdot \text{cm}^{-3} \quad (3)$$

where M is the molecular mass of $Co_{0.5}Zn_{0.5}Fe_2O_4$ (g/mol), N = Avogadro's number (6.022×10^{23} entities/mol), and "a" is the lattice constant (cm).

Calculated result presented in **Table 2** showed that the density is in close agreement with published data (JCPDS, 1971 and JCPDS, 1947). As temperature increases, the density of the sample also increases for both the calculated and measured densities as shown in **Figure 2**.

The crystallite size as a function of sintering temperature is presented in **Table 3** and interpreted in **Figure 3**. The crystallite size of the sintered as powdered was calculated using the Scherer relationship from the XRD lines. The full wave half maximum, (FWHM) value was converted to radian before computation in the Scherer equation. The conversion from degree to radian for the FWHM value was done by using the formula [12];

$$\text{radian} = \frac{\beta \times 2\pi}{360} \quad (4)$$

where β is the FWHM value in degree, π is 3.142.

The crystallite size calculated for the $Co_{0.5}Zn_{0.5}Fe_2O_4$ powder sample sintered at different temperatures of 500˚C, 700˚C, 900˚C, and 1100˚C produced values in the range of 21.43 - 63.38 nm. Result showed that the milled sample (without sintering) has already showed a distinct diameter from the rest of the sintered diameter.

Table 1. Intensity and 2Theta for samples sintered at different temperatures.

Temperature (˚C)	2Theta (deg)	Intensity (a.u)
0	35.491	935.86
500	35.423	4072.02
700	35.505	4965.12
900	35.431	7256.39
1100	35.615	7571.93

Table 2. Density of samples at different sintering temperature.

Temperature (˚C)	Compound	Molecular mass (g/mole)	Calculated density (g/cm^{-3})	Measured density (g/cm^{-3})
0	$Co_{0.5}Zn_{0.5}Fe_2O_4$	237.85	5.33	5.32
500	✓	237.85	5.34	5.33
700	✓	237.85	5.35	5.34
900	✓	237.85	5.36	5.36
1100	✓	237.85	5.41	5.40

Table 3. Crystallite size of $Co_{0.5}Zn_{0.5}Fe_2O_4$ sample sintered at different temperatures.

Temperature (˚C)	FWHM (deg)	Crystal size (nm)
0	0.3897	21.43
500	0.1948	42.86
700	0.1624	52.05
900	0.1299	63.35
1100	0.1299	63.38

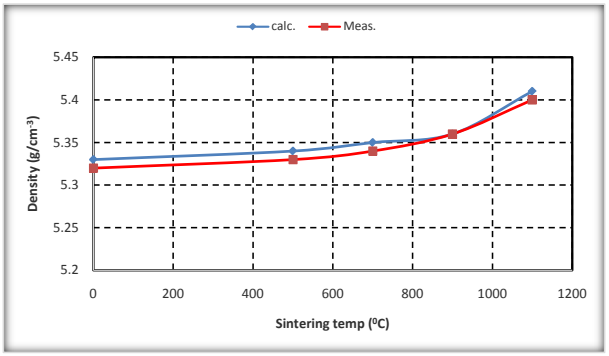

Figure 2. Variation in measured and calculated density of MUT.

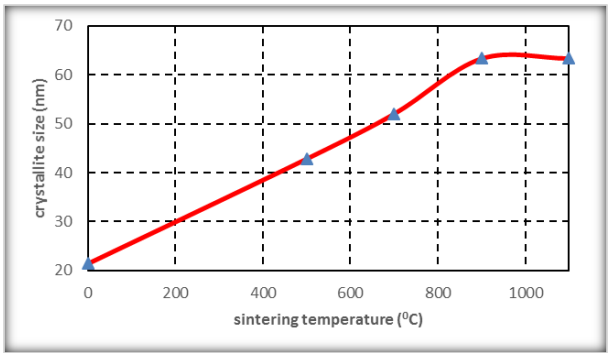

Figure 3. Crystallites of sample vs sintering temperature.

Growth of particles is observed from 500˚C to 1100˚C, this is due to the mechanical alloy method used in the preparation of the sample. As the temperature increases, a broader particle size begins to emanate due to the thermal energy supplied at this stage. Grain growth development started at above the 700˚C, where necking process starts to appear. The grain distribution at 1100˚C is wider than that of the 700˚C which is attributed to grain growth to larger sizes thereby creating more development of domain walls.

Scanning electron microscope (SEM) micrographs of $Co_{0.5}Zn_{0.5}Fe_2O_4$ particles sintered at different temperatures for 10 hours in air synthesised via mechanical alloy method is presented in **Figure 4**. The result from SEM analysis showed that the surface microstructure of sintered $Co_{0.5}Zn_{0.5}Fe_2O_4$ are bundle together with increasing sintering temperature from 500˚C to 1100˚C. It was also observed that the average grain size increased with increasing sintering temperature.

Energy dispersive X-ray (EDX) analysis was performed to confirm quantitative composition of elements in the $Co_{0.5}Zn_{0.5}Fe_2O_4$ nano particles after sintering at different temperatures. Result from the analysis as shown in **Table 4** confirmed that the stoichiometric composition of mixture before sintering was also the same after sintering.

TEM micrograph shown in **Figure 5** is of the ferrite powder obtained from the milling process and sintered at different temperatures. Samples to be studied were sonificated in acetone and dispersed uniformly on the TEM copper grid. The TEM micrograph revealed difference in size distribution as temperature changes. The particle size distribution obtained from TEM micrographs from **Figure 5** showed that the average particles sizes are 18.0 nm, 20 nm, 39.5 nm, 48.5 nm, and 57.5 nm for the unsintered, 500˚C, 700˚C, 900˚C, and 1100˚C respectively.

4. Conclusion

Co-Zn ferrite nano powders were synthesized using the mechanical alloying method with a molar ratio of 1:0.5:0.5. The XRD spectra indicate the diffusion of ZnO into the tetrahedral sites followed by CoO into the octahedral sites. The diffusion occurred during the early stage of the milling process. The crystal size calculated exhibits an increase in nano dimension due to the sintering process with a corresponding increase in density of

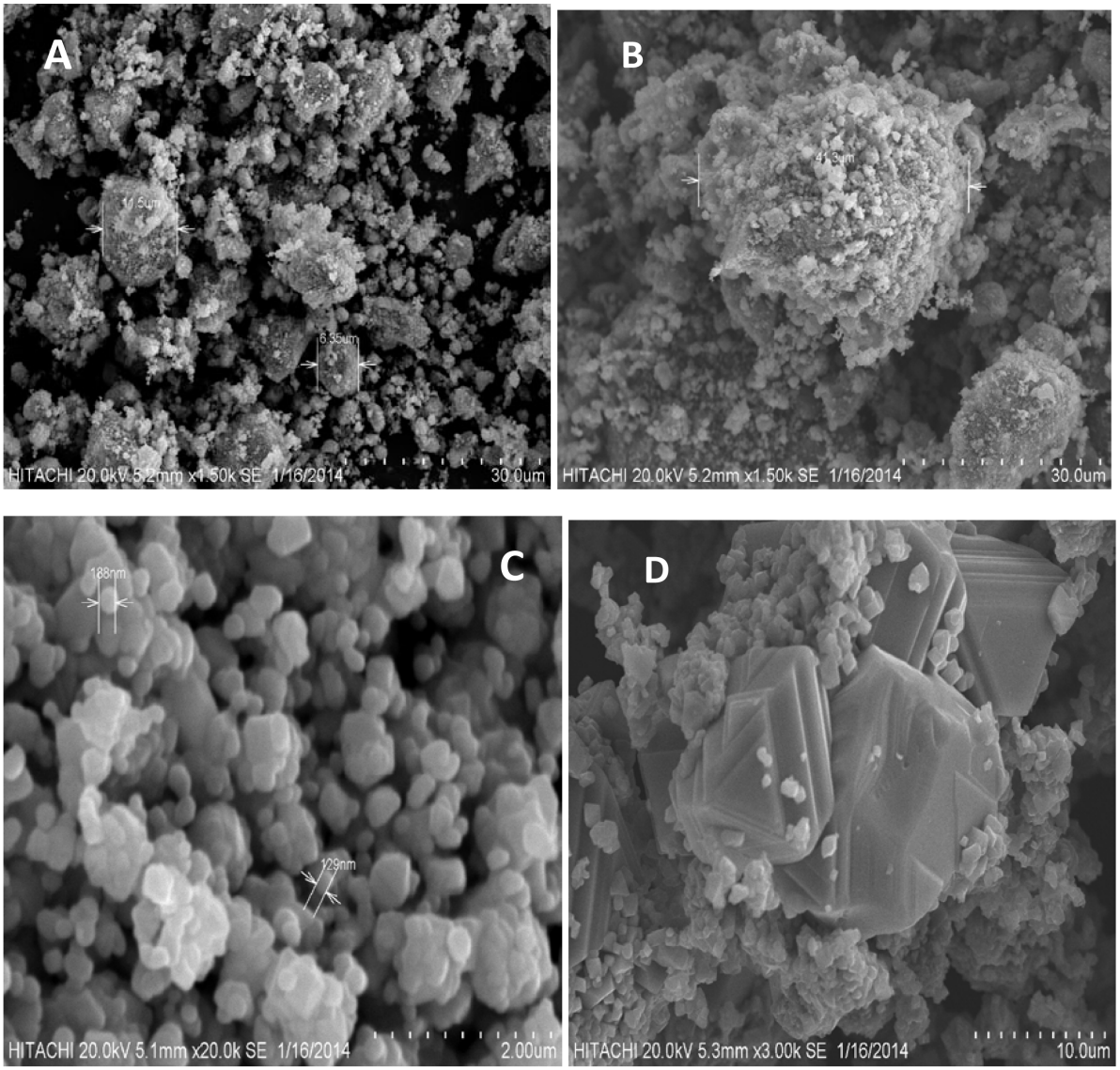

Figure 4. SEM micrograph of $Co_{0.5}Zn_{0.5}Fe_2O_4$ nano particles sintered at (A) 500˚C (B) 700˚C (C) 900˚C and (D) 1100˚C.

Table 4. Elemental composition of the $Co_{0.5}Zn_{0.5}Fe_2O_4$ sintered powder at 500˚C.

Element line	Weight %	Weight % error	Atom %	Atom % error	Compnd %	Norm. compnd%
O K	32.99	+/−0.32	63.85	+/−0.61	32.99	32.99
Fe K	48.19	+/−0.46	26.72	+/−0.25	48.19	48.19
Fe L	---	---	---	---	---	---
Co K	9.90	+/−0.40	5.20	+/−0.21	9.90	9.90
Co L	---	---	---	---	---	---
Zn K	8.93	+/−0.44	4.23	+/−0.21	8.93	8.93
Zn L	---	---	---	---	---	---
Total	100.00		100.00		100.00	100.00

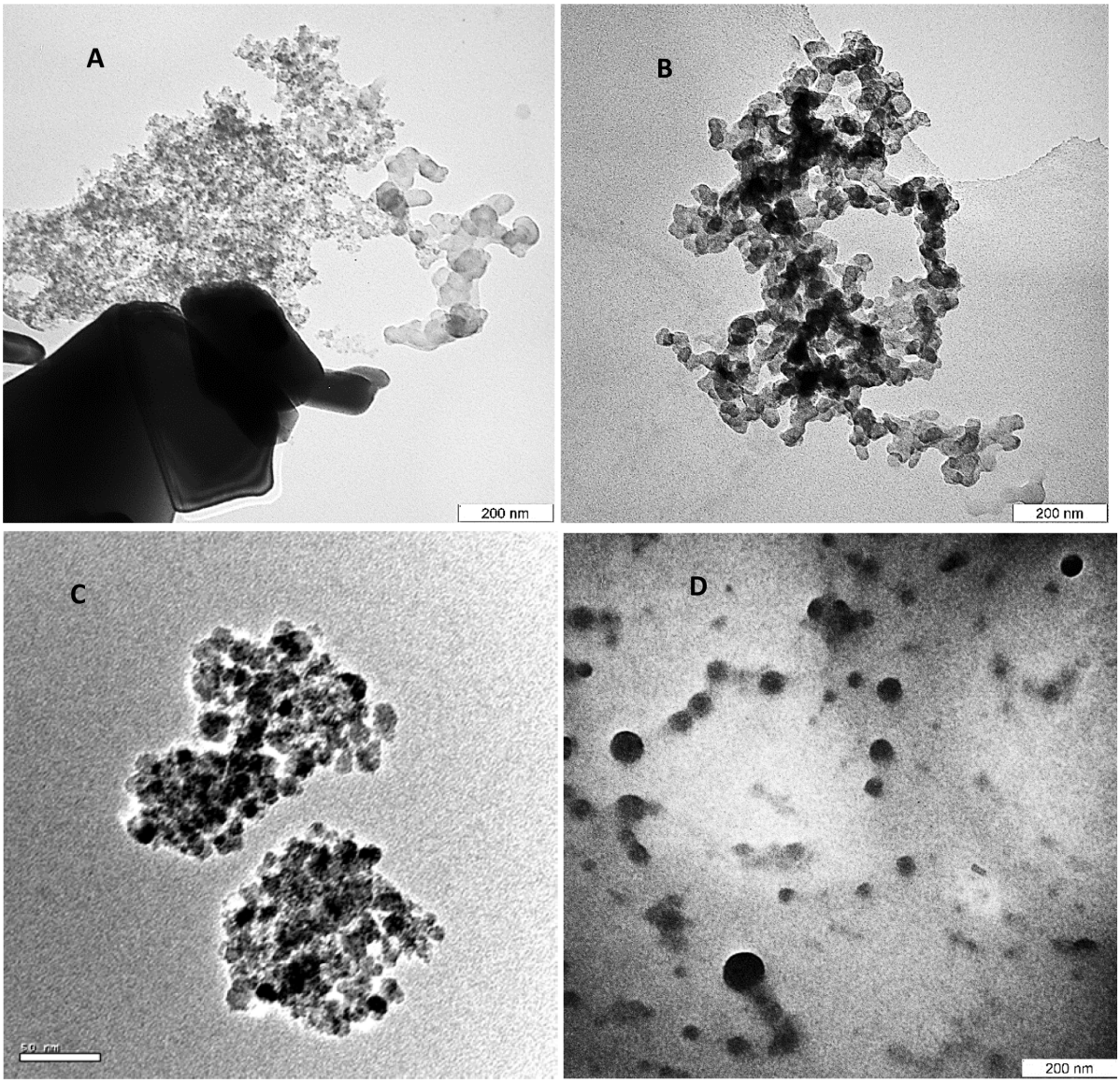

Figure 5. TEM micrograph of $Co_{0.5}Zn_{0.5}Fe_2O_4$ nano particles sintered at (a) 500˚C (b) 700˚C (c) 900˚C and (D) 1100˚C.

the samples. This behaviour is also evident from the SEM analysis showing increase in compactness of the samples as temperature increases. The micrograph of SEM showed that the synthesized powders began to agglomerate as the sintering temperature increases. TEM micrograph showed that the powders are of nanosize dimension and the values of the sizes increase with increasing sintering temperature.

Acknowledgements

The researchers wish to thank the Universiti Putra Malaysia for the fund provided under grant Vot no. 5526200.

References

[1] Ismayadi, I., Hashim, H., Khamirul, A.M. and Alias, R. (2009) The Effect of Milling Time on $Ni_{0.5}Zn_{0.5}Fe_2O_4$ Compositional Evolution and Particle Size Distribution. *American Journal of Applied Sciences*, **6**, 1548-1552. http://dx.doi.org/10.3844/ajassp.2009.1548.1552

[2] Pandu, R., Yadav, K.L., Kumar, A., Reddy, P.R. and Gupta, A.V.S.S.K.S. (2010) Effect of Sintering Temperature on Structural and Electrical Properties of BiFeO3 Multiferroics. *Indian Journal of Engineering and Materials Sciences*, **17**,

481-485.

[3] Bhuiyan, M.A., Hoque, S.M. and Choudhury, S. (2010) Effects of Sintering Temperature on Microstructure and Magnetic Properties of $NiFe_2O_4$ Prepared from Nano Size Powder of NiO and Fe_2O_3. *Journal of Bangladesh Academy of Sciences*, **34**, 189-195.

[4] Bafrooei, H.B., Nassaj, E.T., Ebadzadeh, T. and Hu, C.F. (2014) Sintering Behavior and Microwave Dielectric Properties of Nano Zinc Niobate Powder. *Ceramics International*, **40**, 14463-14470. http://dx.doi.org/10.1016/j.ceramint.2014.07.019

[5] Okazaki, Y., Lixin, M., Ohya, Y., Yanase, S. and Hashi, S. (2007) Magnetic Properties of Nanocrystalline Ferrite $Ti_xCo_{1+x}Fe_{2-2x}O_4$ and $CoFe_2O_4$ Composite Thin Films. *Journal of Materials Processing Technology*, **181**, 66-70. http://dx.doi.org/10.1016/j.jmatprotec.2006.03.010

[6] Gul, I.H., Abbasi, A.Z., Amin, F., Anis-ur-Rehman, M. and Maqsood, A. (2007) Structural, Magnetic and Electrical Properties of $Co_{1-x}Zn_xFe_2O_4$ Synthesized by Co-Precipitation Method. *Journal of Magnetism and Magnetic Materials*, **311**, 494-499. http://dx.doi.org/10.1016/j.jmmm.2006.08.005

[7] Islam, R., Rahman, M.O., Hakim, M.A., Saha, D.K., Saiduzzaman, S., Noor, S. and Al-Mamun, M. (2012) Effect of Sintering Temperature on Structural and Magnetic Properties of Ni0. 55Zn0. 45Fe2O4 Ferrites. *Materials Sciences and Applications*, **3**, 326. http://dx.doi.org/10.4236/msa.2012.35048

[8] Hou, P.Y., Paulikas, A.P. and Veal, B.W. (2004) Growth Strains and Stress Relaxation in Alumina Scales during High Temperature Oxidation. *Materials Science Forum*, **461**, 671-680. http://dx.doi.org/10.4028/www.scientific.net/MSF.461-464.671

[9] Bousquet, M., Viala, B., Achard, H., Georges, J., Reinhardt, A. and Le Rhun, A. (2014) Pt-Less Silicon Integration of PZT Sol-Gel Thin Films. *Conference on Application of Polar Dielectrics*, Lithuania.

[10] Yakubu, A., Abbas, Z., Hashim, M. and Fahad, A. (2014) Effect of Milling Time on $Co_{0.5}Zn_{0.5}Fe_2O_4$ Microstructure and Particles Size Evolution via the Mechanical Alloying Method. *Journal of Materials Science and Chemical Engineering*, **2**, 58-63. http://dx.doi.org/10.4236/msce.2014.211008

[11] JCPDS (1971) Joint Committee on Powder Diffraction Standards (JCPDS), JCPDS (card no: 00-022-1086).

[12] Scherrer, P. (1918) Bestimmung der Grösse und der Inneren Struktur von Kolloidteilchen Mittels Röntgenstrahlen, Nachrichten von der Gesellschaft der Wissenschaften, Göttingen. *Mathematisch-Physikalische Klasse*, **2**, 98-100

[13] Hossein, A.K.M.A., Mahmud, S.T., Seki, M., Kawai, T. and Tabata, H. (2006) Structural, Electrical Transport, and Magnetic Properties of $Ni_{1-x}Zn_xFe_2O_4$. *Journal of Magnetism and Magnetic Materials*, **312**, 210-219. http://dx.doi.org/10.1016/j.jmmm.2006.09.030

[14] Ismayadi, I. (2012) Parallel Evolving Morphology, Magnetic Properties and Their Relationships in $Ni_{0.5}Zn_{0.5}Fe_2O_4$. Ph.D. Thesis, Universiti of Putra, Malaysia.

[15] Yousefi, M.H., Manouchehri, S., Arab, A., Mozaffari, M., Amiri, Gh.R. and Amighian, J. (2010) Preparation of Cobalt-Zinc Ferrite ($Co_{0.8}Zn_{0.2}Fe_2O_4$) Nanopowder via Combustion Method and Investigation of Its Magnetic Properties. *Materials Research Bulletin*, **45**, 1792-1795.

[16] Heiroth, S., Frison, R., Rupp, J.L., Lippert, T., Barthazy Meier, E.J., Müller Gubler, E. and Gauckler, L.J. (2011) Crystallization and Grain Growth Characteristics of Yttria-Stabilized Zirconia Thin Films Grown by Pulsed Laser Deposition. *Solid State Ionics*, **191**, 12-23. http://dx.doi.org/10.1016/j.ssi.2011.04.002

[17] Guan, B.H., Chuan, L.K. and Soleimani, H. (2014) Synthesis, Characterization and Influence of Calcinations Temperature on Magnetic Properties of $Ni_{0.75}Zn_{0.25}Fe_{2O}4$ Nanoparticles Synthesized by Sol-Gel Technique. *American Journal of Applied Sciences*, **11**.